Synthesis and Characterization of Polystyrene/Layered Double-Hydroxide Nanocomposites via *In Situ* Emulsion and Suspension Polymerization

Peng Ding, Baojun Qu

State Key Laboratory of Fire Science and Department of Polymer Science and Engineering, University of Science and Technology of China, Hefei, Anhui 230026, People's Republic of China

Received 14 July 2005; accepted 16 October 2005
DOI 10.1002/app.23447
Published online in Wiley InterScience (www.interscience.wiley.com).

ABSTRACT: Polystyrene (PS)/ZnAl layered double-hydroxide (LDH) nanocomposites were synthesized via *in situ* emulsion and suspension polymerization in the presence of *N*-lauroyl-glutamate surfactant and long-chain spacer and characterized with elemental analysis, Fourier transform infrared spectrum, X-ray diffraction (XRD), transmission electron microscopy (TEM), and thermogravimetric analysis. The XRD and TEM results demonstrate that the exfoliated ZnAl–LDH layers were well dispersed at molecular level in the PS matrix. The completely exfoliated PS/LDH nanocomposites were obtained even at the 20 and 10 wt % LDH loadings prepared by emulsion polymerization and suspension polymerization, respectively. The PS/LDH nanocomposites with a suitable amount of LDH showed apparently enhanced thermal stability. When the 50% weight loss was selected as a comparison point, the decomposition temperature of the exfoliated PS/LDH sample prepared by emulsion polymerization with a 5 wt % LDH loading was about 28°C higher than that of pure PS. © 2006 Wiley Periodicals, Inc. J Appl Polym Sci 101: 3758–3766, 2006

Key words: nanocomposites; emulsion polymerization; polystyrene; thermal properties

INTRODUCTION

Recently, polymer/layered inorganic nanocomposites (PLNs) have attracted great interest in the field of material chemistry because of their novel mechanical, thermal, and optical properties.[1–5] Several methods have been reported for the synthesis of PLNs with good properties, including solution blending, melt blending, and *in situ* preparation.[6] Among these methods, *in situ* polymerization of monomers, especially emulsion and suspension polymerization, has been proved as a new and efficient method for the synthesis of PLNs in recent years. Several PLN systems have been successfully synthesized via *in situ* polymerization, for example, poly(methyl methacrylate) (PMMA)/montmorillonite (MMT), polystyrene (PS)/MMT, polyacrylonitrile/MMT, and PS/graphite oxide.[2,7–13]

Nowadays, polymer/layered double-hydroxide (LDH) nanocomposites have become an emerging class of materials; they may be used as flame retardants, stabilizers, medical materials, and so on.[14] Polymer/LDH nanocomposites can be divided into two main types, intercalated nanocomposites and exfoliated nanocomposites, according to the different dispersion state of the LDH layers in the polymer framework. Of course, there exists a partially exfoliated state in some systems, namely, intercalated–exfoliated structure. In the previous types, the exfoliated polymer/LDH nanocomposites usually attract most interest because they have a molecular dispersion of high-aspect-ratio LDH layers in polymer nanocomposites and thus give some improved properties over microdispersed and conventional composites.[8] Several synthesis methods have been used to prepare exfoliated polymer/LDH nanocomposites, including polyethylene-grafted-maleic anhydride/MgAl–LDH (LDH in which the metal cations are Mg^{2+} and Al^{3+}) exfoliated nanocomposites with up to 5 wt % LDH loading synthesized by the refluxing of MgAl–LDH in a xylene solution of polyethylene-grafted-maleic anhydride.[15] Poly(styrene sulfonate)/ZnAl–LDH (LDH in which the metal cations are Zn^{2+} and Al^{3+}) exfoliated nanocomposites were prepared by an exchange and template reaction in aqueous media.[16] However, as far as we are aware, among all of the aforementioned methods used for synthesis of PLNs, only the *in situ* polymerization method has not been successfully applied to the synthesis of exfoliated polymer/LDH nanocom-

Correspondence to: B. Qu (qubj@ustc.edu.cn).
Contract grant sponsor: National Natural Science Foundation of China; contract grant number: 50373039.
Contract grant sponsor: China National Key Basic Research Special Funds (NKBRSF) project; contract grant number: 2001 CB409600.

posites up to now. This may be due to the unique structures and natural characters of LDHs. LDHs are layered materials constituted by the stacking of positive hydroxylated layers $[M^{2+}_{1-x}M^{3+}_{x}(OH)_2]^{x+}$ separated by interlayered anionic species and water molecules $[X^{q-}_{x/q} \cdot nH_2O]$, where M^{2+} and M^{3+} are divalent and trivalent metal cations, respectively; X^{q-} is the interlayer anion; and x is the molar ratio of M^{2+} to M^{3+}. They are well known for their unique anion-exchange properties and their rich chemistry. The high charge density of the LDHs layers and the high content of anionic species and water molecules result in strong interlayer electrostatic interactions between the sheets and significantly hydrophilic properties. Such dense interlamellar hydrogen bonding networks lead to a tight stacking of the lamellae. The rigid spheroidal sand rose morphology of intergrown platelets prevents both swelling and exfoliation of the sheets in water, wherein the swelling or exfoliation is one of the key factors for the preparation of exfoliated PLNs.[17] Thus, it is a challenge to eliminate the stronger electrostatic interactions between LDH layers in an aqueous system and successfully synthesize exfoliated polymer/LDH nanocomposites via *in situ* polymerization.

In this article, we report the synthesis and characterization of PS/ZnAl–LDH nanocomposites via *in situ* emulsion and suspension polymerization with two different surfactants, *N*-lauroyl-glutamate (LG) and commonly used sodium dodecyl sulfate (SDS), and a long-chain spacer. We found for the first time that the LDH layers could be completely exfoliated in the nanocomposites even at a content of ZnAl–LDH as high as 20 wt % with emulsion polymerization and 10 wt % with suspension polymerization. The PS/LDH nanocomposites with a suitable amount of LDH showed apparently enhanced thermal stability.

EXPERIMENTAL

Materials

n-Hexadecane were purchased from Damao Chemical Reagent Corp (Tianjin, China). LG was supplied by Leasun Chemical Regent Co., Ltd (Shanghai, China). The other chemicals, including $Zn(NO_3)_2 \cdot 6H_2O$, $Al(NO_3)_3$, NaOH, potassium persulfate ($K_2S_2O_8$), sodium sulfite (Na_2SO_3), benzoyl peroxide (BPO), ethyl ether, SDS, and styrene, were obtained from China Medicine (Group) Shanghai Chemical Reagent Corp (Shanghai, China). Styrene was first washed with NaOH solution to remove the inhibitor and then with water and was then distilled under reduced pressure. $K_2S_2O_8$, Na_2SO_3, and BPO were recrystallized. All of the other chemicals were used as received without further purification. Distilled water was used throughout.

Preparation

Polymerization with LG

LG (1.15 g) and *n*-hexadecane (3 g) were mixed in 12 mL of water at 40°C under stirring to form a transparent solution. Then, 11 mL of Zn–Al salt solution, in which the concentration molar ratio of $Zn(NO_3)_2 \cdot 6H_2O$ and $Al(NO_3)_3$ was 3:1, and 15 mL of 1 mol/L NaOH solution were simultaneously added into the previous solution with the help of a peristaltic pump working at a discharge of about 2 mL/min. The pH value of the system was adjusted to a range of 9.5–10. Then, styrene at a calculated amount was added to form an emulsion. Finally, initiators were added to initiate polymerization at 80°C for 6 h in an oil bath, where in the case of emulsion polymerization, the initiators were $K_2S_2O_8$ and Na_2SO_3, and in the case of suspension polymerization, the initiator was BPO. The prepared PS/ZnAl LDH nanocomposites were precipitated in methanol; filtered; thoroughly washed with ethyl ether to remove the *n*-hexadecane and then alcohol and water; and dried at 80°C to obtain PS/LDH powders with different LDH loadings. The samples were labeled E-LG-Hx-*y* or S-LG-*y*, where E represents the emulsion method, S represents the suspension method, LG represents LG surfactant, H represents *n*-hexadecane, *x* represents the dosage of *n*-hexadecane, and *y* represents the content of LDH loading. For comparison, pure PS (without LDH loading) and ZnAl–LG (with 100 wt % LDH loading) were also synthesized with the previous method.

Polymerization with SDS

$Zn(NO_3)_2 \cdot 6H_2O$ (2.23 g), $Al(NO_3)_3$ (0.94 g), SDS (2.22 g), and *n*-hexadecane (3 g) were mixed in 90 mL of water. NaOH (1 mol/L) solution was simultaneously added until the pH value was adjusted to the range 9.5–10. Then, styrene was added to form a uniform solution. Finally, initiators were added to initiate polymerization at 80°C for 6 h in an oil bath. The prepared PS/ZnAl–LDH nanocomposites were treated as described previously to obtain the PS/LDH powders. The samples were labeled E-SDS-*y* or S-SDS-*y*, where SDS represents SDS surfactant. For comparison, ZnAl–SDS (with 100 wt % LDH loading) samples were also synthesized with the same method.

Characterization

Zn elemental analysis was performed on an Autoscan Advantage ICP-AES analyzer (Thermo Javvell Ash Co, Franklin, MA). The Fourier transform infrared (FTIR) spectrum was recorded on a Nicolet MAGNA-IR 750 spectrometer (Nicolet Instrument Co., Madison, Wisconsin, USA). The X-ray diffraction (XRD) data were recorded at room temperature on a Philips X'

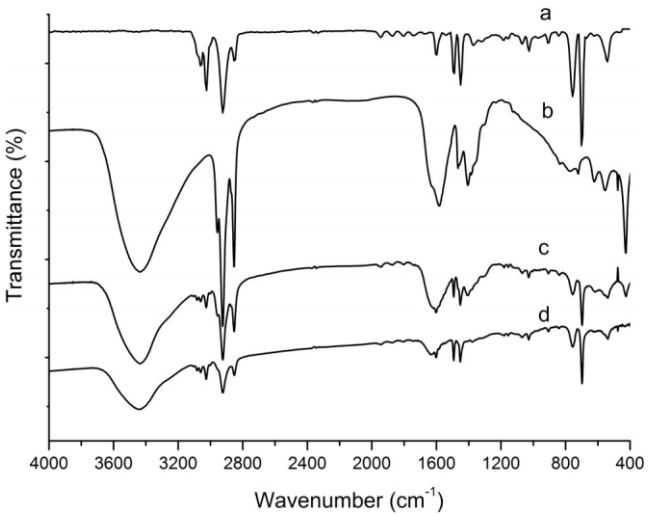

Figure 1 FTIR spectra of the samples: (a) PS, (b) ZnAl–LG, and the PS/LDH nanocomposites (c) E-LG-H1-10 and (d) S-LG-10.

Pert PRO SUPER apparatus (Panalytical Co., Almelo, Netherlands) with Cu Kα radiation with a Ni filter (wavelength = 1.5418 Å) at a scanning rate of 0.0167°/s. The transmission electron microscopy (TEM) images were obtained on a Hitachi H-800 transmission electron microanalyzer (Hitachi, Ltd., Tokyo, Japan) with an acceleration voltage of 200 kV. The samples were ultramicrotomed with a diamond knife on an LKB Pyramitome (LKB Instruments, Inc., Gaithersburg, MD) to give 100-nm thick slices. The slices were transferred from water to a Cu grid. The thermogravimetric analyses (TGAs) were performed on a Shimadzu TGA-50H thermoanalyzer (SHIMADZU Co., Kyoto, Japan). The samples were examined under an air flow rate of 2×10^{-5} m^3/min at a scanning rate of 10°C/min. The molecular weights of the samples were determined from viscosity measurement carried out as following. First, the nanocomposites were solved in tetrahydrofuran and filtered to obtain polymer free of the LDH. Then, the viscosity measurements were performed. Finally, the molecular weights were calculated from the result, which was an average of three viscosity determinations, and Mark–Houwink constants were obtained from published data.[18]

RESULTS AND DISCUSSION

Characterization of the PS/LDH samples

The contents of LDH in the samples were determined by the elemental analysis. The results show that the LDH loadings were in agreement with the designed contents. For example, the Zn contents in the E-LG-H1-y series samples with different ZnAl–LDH loadings were determined as 0.375, 4.35, and 12.2 wt %, respectively, corresponding to $[Zn_3Al(OH)_8](LG)_{0.5}$ contents of about y = 1, 10, and 30 wt %, respectively.

Figure 1 shows the typical FTIR spectra of PS, ZnAl–LG, and PS/LDH samples prepared by emulsion and suspension polymerization with LG surfactant. The pure PS [Fig. 1(a)] had several characteristic absorption bands at 3100–2800 cm^{-1} (C—H stretching vibration), 2000–1680 cm^{-1} (weak aromatic overtone and combination band), 1604 and 1496 cm^{-1} (C═C stretching vibration), 1453 and 1368 cm^{-1} (CH_2 bending vibrations), 757 and 698 cm^{-1} (CH out-of-plane bending of the phenyl ring), and 540 cm^{-1} (out-of-plane deformation of the phenyl ring). FTIR spectroscopy of the ZnAl–LG samples [Fig. 1(b)] showed broad absorption bands around 3500 and 1630 cm^{-1} due to O—H stretching of the hydroxyl groups of LDH and corresponding δ(H—OH) vibration, respectively. The M—O and O—M—O (M = Zn or Al) vibration bands appear in the 400–800-cm^{-1} region. The presence of LG was confirmed by the C—H stretching vibration at 2957, 2923, and 2853 cm^{-1} and the N—H bending vibration of the RCONH— group at 1582 cm^{-1}. Obviously, the FTIR spectra of the PS/LDH samples [Fig. 1(c,d)] showed the combination of the characteristic absorption bands in Figure 1(a,b), which provided evidence that the LDH layers were doped into the PS matrix.

Figure 2 shows the FTIR spectra of PS, ZnAl–SDS, and PS/LDH samples prepared by emulsion and suspension polymerization with SDS surfactant. The results are similar to those shown in Figure 1. Figure 2(b) shows evidence of the presence of SDS instead of NO_3^- in the ZnAl–SDS sample by the C—H stretching vibration at 2848, 2920, and 2957 cm^{-1} and the stretching vibration of sulfate at 1218 and 1247 cm^{-1}. The

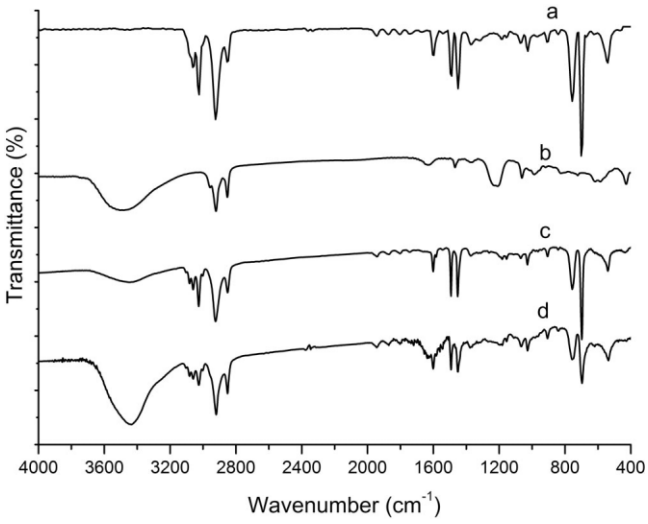

Figure 2 FTIR spectra of the samples: (a) PS, (b) ZnAl–SDS, and the PS/LDH nanocomposites (c) E-SDS-5 and (d) S-SDS-5.

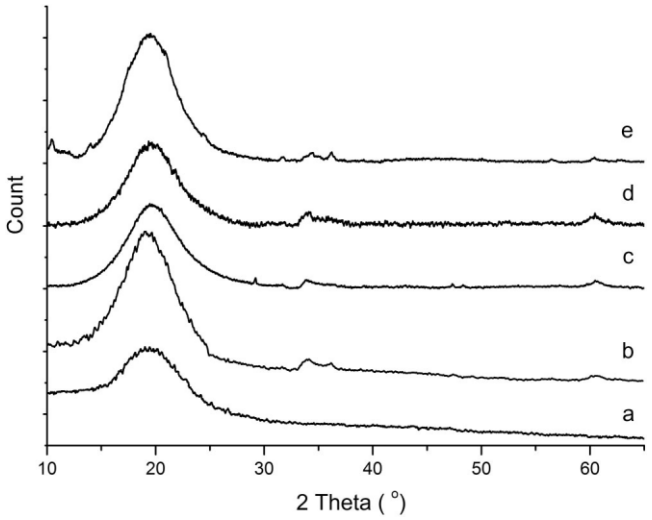

Figure 3 Wide-angle XRD pattern of (a) pure PS and the PS/LDH samples (b) E-LG-H1-10, (c) E-SDS-5, (d) S-LG-10, and (e) S-SDS-5.

FTIR spectra of the PS/LDH samples [Fig. 2(c,d)] showed the combination of the characteristic absorption bands in Figure 2(a,b), which indicated that the LDH layers were dispersed into the PS matrix to form the PS/LDH composites.

Further evidence for the presence of LDH in the PS matrix was obtained from the XRD patterns recorded for the PS/LDH samples. Figure 3 compares the typical wide-angle XRD patterns of pure PS and different PS/LDH samples. Several new peaks were found in the patterns of PS/LDH samples, wherein the peak at $2\theta = 60°$ was indexed as (110) in a hexagonal lattice with a 3R stacking sequence of the LDH sheets. This indicates that the layered framework is preserved in the PS matrix. Similar results have been found in the literature.[19]

The results obtained by the elemental analysis, FTIR, and XRD give positive evidence that the LDH layers were dispersed into the PS matrix.

Intercalated/exfoliated structures of the PS/LDH nanocomposites

Low-angle XRD was often used to characterize the types of the layered structures, that is, intercalated and/or exfoliated polymer/LDH nanocomposites because the peaks changed with the gallery height of the LDH. Figure 4 gives the low-angle XRD patterns of the PS/LDH samples, which indicates the different structures of PS/LDH nanocomposites prepared by different methods and surfactants. No peaks at $2\theta = 1.5–10°$ were observed in Figure 4(a–c), which indicated the exfoliated structures of these PS/LDH nanocomposites. On the other hand, Figure 4(d,e) shows two peaks in the range of less than 10°, corresponding to d values of 2.52 and 1.26 nm, respectively. This means the intercalated structures existed in the PS/LDH nanocomposites.[19]

Figure 5 gives the images recorded by TEM analysis of the samples. Figure 5(a) presents the TEM image of the E-LG-H1-1 sample with 1 wt % LDH loading. The LDH layers [the dark part in Fig. 5(a)] combined with LG surfactants were homogeneously dispersed in the PS matrix (bright part). Moreover, this TEM micrograph was very different from those of polymers/layered silicates exfoliation nanocomposites, in which the exfoliated clay layers are often face–face orientated because of the very high aspect ratio.[20] In the case of the exfoliated nanocomposite sample, the exfoliated LDH sheets combined with surfactants were dispersed disorderly in the PS matrix and mostly parallel to the grid, which was in good agreement with our previous work.[15] The arrow on the image points to one of the individual exfoliated layers, which shows that the thickness and lateral sizes of the exfoliated LDH layers were about 1 and 70–100 nm, respectively. Figure 5(b) shows the corresponding high-resolution transmission electron microscopy (HR-TEM) image of Figure 5(a), which permitted a more clear observation of the dispersion and exfoliation state of the LDH layers. Apparently, almost all of the LDH layers were laid parallel to the Cu grid and only partially overlapped each other. These kinds of completely exfoliated structures were in good agreement with the XRD data shown in Figure 4(a).

The HR-TEM image [Fig. 5(c)] of the S-LG-10 sample prepared by suspension polymerization with 10% LDH loading indicated the 30–50 nm lateral sizes of the LDH layers and the similar dispersion state of LDH layers in PS matrix with that of the E-LG-H1-1 sample, which gave positive evidence of the exfolia-

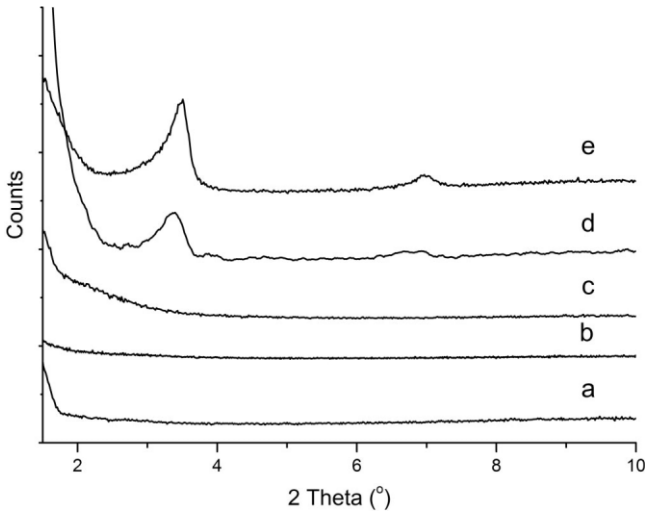

Figure 4 Low-angle XRD pattern of the PS/LDH samples (a) E-LG-H1-1, (b) E-LG-H1-10, (c) S-LG-10, (d) E-SDS-5, and (e) S-SDS-5.

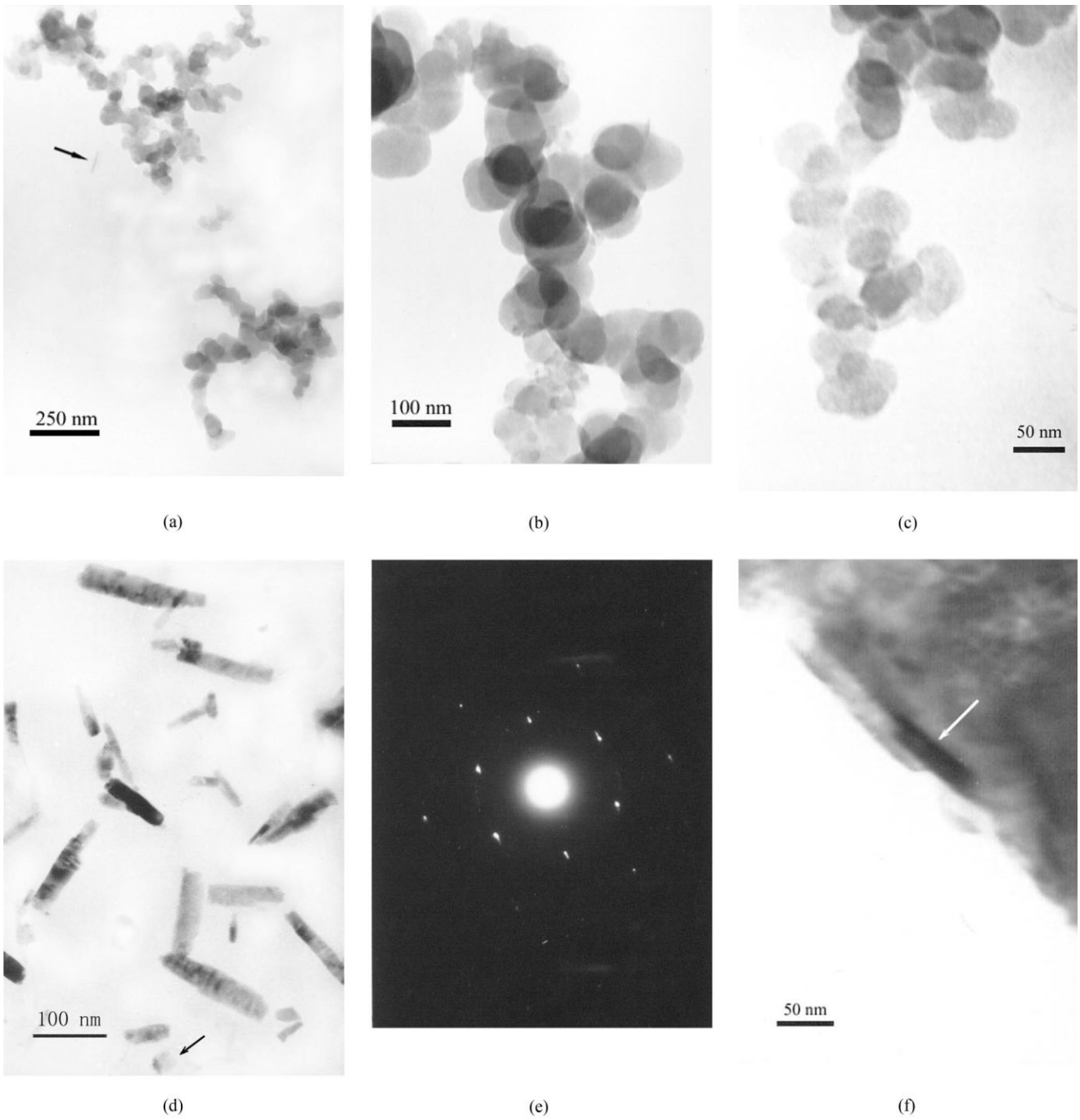

Figure 5 (a) TEM image and (b) corresponding HR-TEM image of the E-LG-H1-1 sample, (c) HR-TEM image of the S-LG-10 sample, (d) TEM image and (e) corresponding ED (selected area electron diffraction) pattern of the E-LG-H1-20 sample, and (f) HR-TEM image of the E-SDS-5 sample.

tion structures, which was in good agreement with the XRD data [see Fig. 4(c)].

Figure 5(d) gives the TEM image of the E-LG-H1-20 sample with 20 wt % LDH loading. The LDH agglomerates (gray ribbons) were homogeneously dispersed in the PS matrix, in which the LDH layers (black lines) were about 1 nm thick, had lateral sizes of 20–40 nm, and were coated by LG surfactants (gray areas). The LDH layers were almost perpendicular to the Cu grid and parallel to each other, which was similar to the TEM images of intercalated structures and quite different from those of the samples with low LDH loadings [Fig. 5(a–c)]. However, this kind of structure could also be considered as exfoliated because the distance of the two adjacent LDH layers was larger than 10 nm, which was much larger than that of the intercalated structures. Such morphology may have been caused by the high LDH content in the sample.

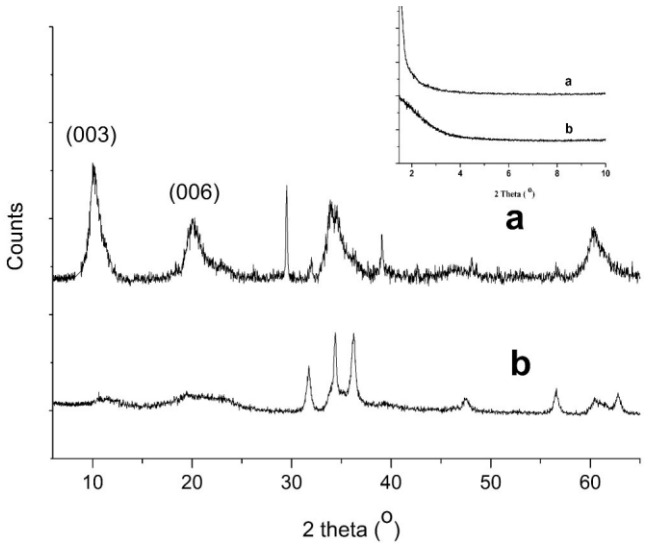

Figure 6 Wide-angle and low-angle (inset) XRD patterns of (a) ZnAl-NO_3 and (b) ZnAl-LG.

The concepts of primary particles and crystallites, according to the literature,[21] were helpful in explaining the submicrometer-sized agglomerates of these exfoliated LDH layers. When at high LDH content in the PS/LDH composite, the random dispersion of LDH layers, or crystallites, with high aspect ratios became more and more hindered because of geometrical constraints within the limited space remaining available in the PS matrix. As a result, the LDH layers could only agglomerate at a certain lever and be arrayed parallel to each other to form the primary particles. However, with careful observation, we found that there were also individual exfoliated layers parallel to the Cu grid, one of which is marked by the arrow in this image. The corresponding ED (selected area electron diffraction) pattern is represented in Figure 5(e), which revealed that the LDH sheets had a hexagonal crystal structure with a crystallographic parameter a of 0.308 nm.

A typical region of the intercalated structure of E-SDS-5 sample with 5 wt % LDH loading prepared by SDS surfactant is shown by the HR-TEM image in Figure 5(f). Apparently, this image indicates several LDH layers were stacked with each other, as shown by the arrow.

To well understand how the exfoliated PS/LDH nanocomposites were obtained in this study, the XRD analysis for some special samples is very helpful. Figure 6 compares the wide-angle and low-angle (inset) XRD patterns of the pristine ZnAl–NO_3 sample with interlayered anions NO_3^- and the dried LG-modified ZnAl–LG sample. The XRD pattern of ZnAl–NO_3 [Fig. 6(a)] could be indexed in a hexagonal lattice with an R-3m rhombohedral symmetry. The refined cell parameters were a = 0.311 nm and c = 2.627 nm ($=3\bullet d_{003}$). Compared with the XRD pattern of the ZnAl–NO_3 sample, the location of some peaks of the ZnAl–LG sample in Figure 6(b) were changed, as observed in our previous work.[15,19] Moreover, these peaks became much broader and weaker, especially for the (003) and (006) peaks, which almost disappeared. The low-angle XRD patterns (inset b of Fig. 6) also showed that a very broad peak appeared at below 3°. All these results indicate that the LDH layers were swollen or even exfoliated with the help of the LG surfactant and long-chain *n*-hexadecane spacers in these systems. Subsequently, when the styrene was added and polymerized, the exfoliated LDH layers were fixed in the PS matrix to form the exfoliated PS/LDH nanocomposites. A similar exfoliation mechanism in the PMMA/MMT nanocomposite system prepared by emulsion polymerization was reported in the literature.[22]

Effects of the preparation methods and LDH contents

Figure 7 gives the low-angle XRD patterns of the PS/LDH samples with different contents of ZnAl–LDH prepared by emulsion polymerization with LG surfactant. No peaks at 2θ = 1.5–10° were observed in Figure 7(a–c), which means that the exfoliated structures of the PS/LDH nanocomposites were obtained when the contents of LDH were less than 20 wt %. However, a very broad peak below 3° appeared in the E-LG-H3-30 sample when the LDH content reached 30 wt % [Fig. 7(d)], which indicated a mixed intercalated–exfoliated structure, as reported previously.[9]

Figures 8 and 9 present similar trends for the PS/LDH samples of the S-LG-*y* and E-LG-H1-*y* series, respectively. As shown by the S-LG-*y* series samples

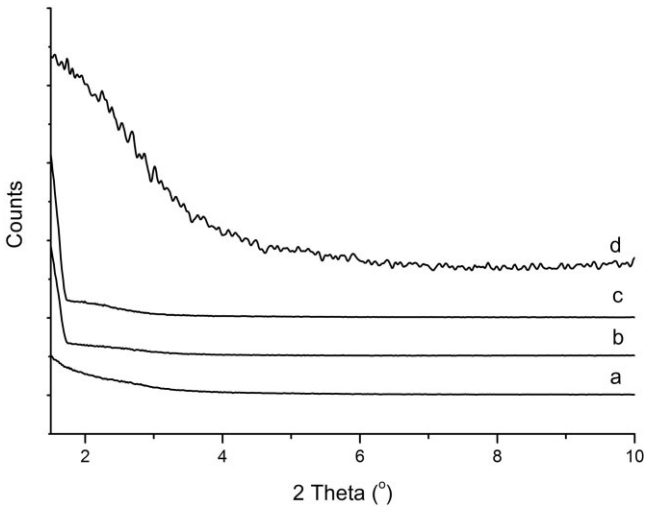

Figure 7 Low-angle XRD pattern of the PS/LDH samples (a) E-LG-H3-5, (b) E-LG-H3-10, (c) E-LG-H3-20, and (d) E-LG-H3-30.

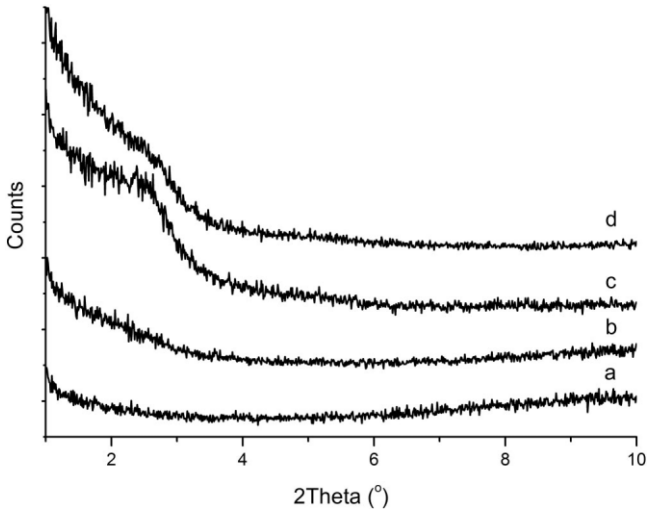

Figure 8 Low-angle XRD pattern of the PS/LDH samples (a) S-LG-5, (b) S-LG-10, (c) S-LG-20, and (d) S-LG-30.

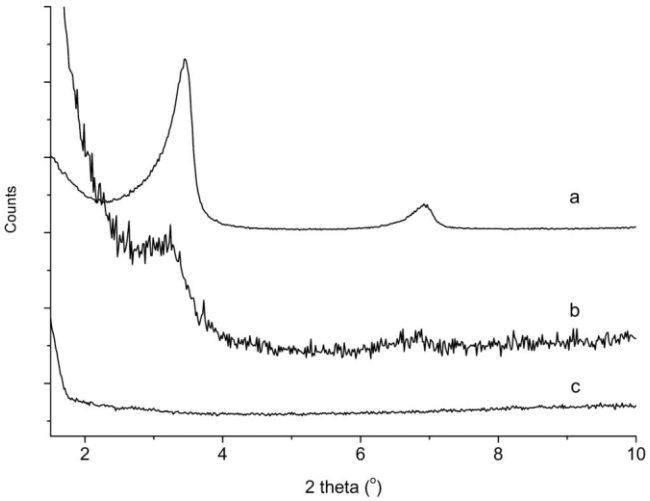

Figure 10 Low-angle XRD pattern of the PS/LDH samples with 5 wt % LDH loading by emulsion polymerization with LG and different spacers: (a) none, (b) 1 g of *n*-octane, and (c) 1 g of *n*-hexadecane.

prepared by suspension polymerization, the exfoliated PS/LDH nanocomposites were obtained when the LDH loadings were less than 10 wt %. That is, the completely exfoliated PS/LDH nanocomposites were prepared by a decrease in the LDH loadings in the PS/LDH nanocomposites. However, the emulsion polymerization method was more efficient than the suspension polymerization in the preparation of the exfoliated PS/LDH nanocomposites, which was reported for the polymer/MMT system.[9]

Effects of the surfactants and spacers

To eliminate the stronger electrostatic interactions between the LDH layers and to obtain the intercalated or exfoliated structures, the surfactants are usually applied to modify the surface property of the LDH layers, which has been proven to be an effective method.[15,23] In this study, two surfactants were used, SDS and LG. At the same time, they were the emulsifiers in the emulsion polymerization. The type of the surfactant had a remarkable effect on the structure of the PS/LDH nanocomposites. When SDS was used as the surfactant, it was very difficult to obtain the exfoliated structure of the nanocomposites because both the E-SDS-5 and S-SDS-5 samples, even only with 5 wt % LDH contents [see Fig. 4(d,e)], showed the two low-angle XRD peaks characteristic of the intercalated structures. On the contrary, however, the LG surfactant was in favor of the exfoliation of the LDH layers in the PS/LDH nanocomposites because the exfoliated structures were obtained even at 20 wt % LDH loading for the emulsion polymerization and at 10 wt % for suspension polymerization, as shown in Figures 7(c) and 8(b), respectively.

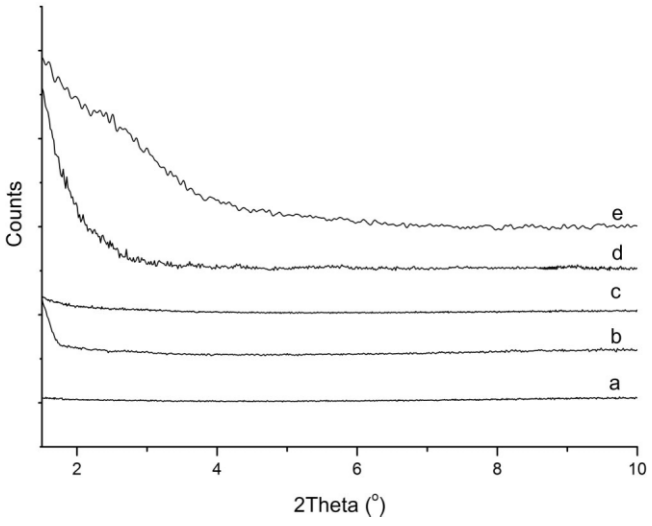

Figure 9 Low-angle XRD pattern of the PS/LDH samples (a) E-LG-H1-1, (b) E-LG-H1-5, (c) E-LG-H1-10, (d) E-LG-H1-20, and (e) E-LG-H1-30.

The spacer also had an important effect on the exfoliation of LDH layers. Figure 10 shows the low-angle XRD patterns of PS/LDH samples with 5 wt % LDH loading prepared by different spacers of short-chain *n*-octane [Fig. 10(b)] and long-chain *n*-hexadecane [Fig. 10(c)] with emulsion polymerization and LG surfactants. For comparison, the low-angle XRD pattern of the PS/LDH sample without a spacer is also shown in Figure 10(a). Two sharp peaks characteristic of an intercalated structure appeared, as shown in Figure 10(a), whereas a broad peak characteristic of an intercalated structure appeared in the sample prepared by short-chain spacer *n*-octane [Fig. 10(b)]. However, only the PS/LDH sample prepared by the long chain spacer *n*-hexadecane had the completely exfoliated

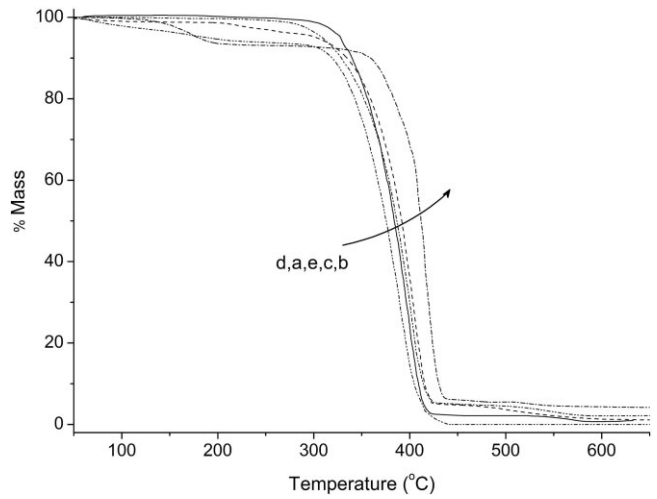

Figure 11 TGA curves of (a) pure PS and the PS/LDH samples (b) E-LG-H1-5, (c) E-SDS-5, (d) S-LG-5, and (e) S-SDS-5.

structure because no peaks appear in Figure 10(c). Thus, it was necessary for the use of long-chain spacers to obtain the completely exfoliated nanocomposites. However, by comparison with Figures 7 and 9, we found that more than 1 g of amount of the spacer had no remarkable effect on the exfoliation of LDH layers.

Thermal properties

Figure 11 shows the TGA curves of pure PS and PS/LDH samples with 5 wt % LDH loading prepared with different methods. The thermal decomposition of the pure PS sample occurred in the range 270–420°C, and no residues were left above 420°C. The first step of weight loss for the PS/LDH samples occurred at about 120–250°C due to the evaporation of physically absorbed water in the intercalated layers, the loss of hydroxide on LDH layers, and the thermal decomposition of the alkyl chains of surfactants. The second step of weight loss took place at the temperature range of 270–450°C due to the thermal decomposition of PS chains and the formation of black charred residues. When 50 wt % weight loss was selected as a point of comparison, the thermal decomposition temperatures for pure PS [Fig. 11(a)] and the PS/LDH nanocomposite samples E-LG-H1-5 [Fig. 11(b)], E-SDS-5 [Fig. 11(c)], S-LG-5 [Fig. 11(d)], and S-SDS-5 [Fig. 11(e)] were determined as 383.8, 411.8, 391.7, 375.3, and 386.5°C, respectively. These data indicate that the E-LG-H1-5 sample had the highest thermal decomposition temperature.

Figure 12 depicts the TGA curves of pure PS and PS/LDH samples prepared by emulsion polymerization with LG surfactant and *n*-hexadecane with different LDH contents, that is, E-LG-H1-*y* series. All curves of the PS/LDH samples showed similar thermal decomposition behaviors as mentioned previously. When 50 wt % weight loss was selected as a point of comparison, the thermal decomposition temperatures for pure PS and the PS/LDH nanocomposite samples containing 1, 5, 10, 20, and 30 wt % LDH were determined as 383.8, 396.9, 411.8, 385.8, 385.7, and 354.7°C, respectively. The thermal decomposition temperature of the PS/LDH samples with 5 and 1 wt % LDH loadings were 28.0 and 13.1°C higher than that of pure PS, respectively. The thermal decomposition temperatures of the PS/LDH samples with 10 and 20 wt % LDH loadings were comparable with that of pure PS. Excess loading of LDH, such as 30 wt %, could lead the thermal stability of the materials to decrease lower than 29.1°C, which was lower than that of pure PS. Among the previous samples, the PS/LDH nanocomposite with 5 wt % LDH loading had the best thermal stability. Such thermal behavior could have been caused by a change in the relative extents of exfoliated LDH layers in the nanocomposites. It has been reported that the beneficial effect of LDH on the thermal stability of polymer matrix is due to the promotion of the charring process of the polymer matrix and the hindered effect of LDH layers for the diffusion of oxygen and volatile products throughout the composite materials during the thermal decomposition of the composites.[15,19] Indeed, at low filler contents, exfoliation dominated, but the amount of exfoliated LDH layers was not sufficient to promote any significant improvement of the thermal stability. A suitable LDH content (5 wt %) increased the amount of exfoliated individual layers and, thus, increased the thermal stability of the nanocomposites. However, when the LDH content further increased to above about 5 wt %, the

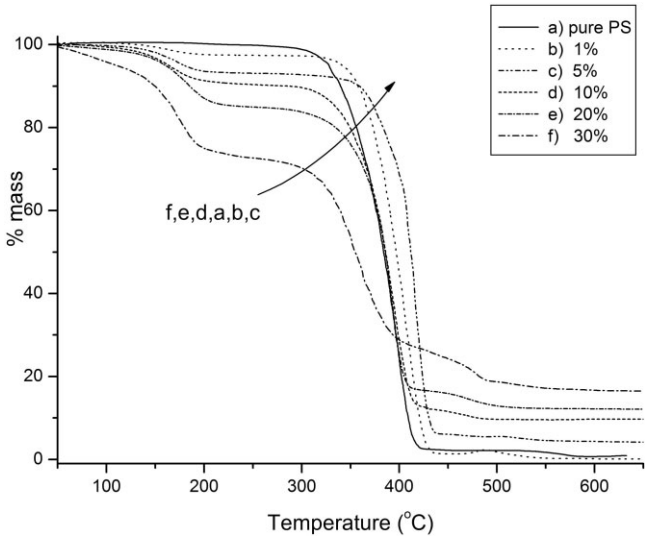

Figure 12 TGA curves of pure PS and E-LG-H1-*y* series samples with different LDH contents.

thermal decomposition temperature did not further increase; it even apparently decreased for the sample with 30 wt % LDH loading. The most probably reason was that the relatively large organic surfactant content of the composites produced less stable charred layers during the decomposition.[24] Very similar behavior has already been observed in some polymer/silicates[1,25] and polymer/LDH[19] nanocomposites.

It is well known that molecular weight has a remarkable influence on the thermal properties of polymers. Therefore, it is necessary to measure the molecular weights of PS in various nanocomposites. The results determined by the viscosity measurement show that the molecular weights of the E-LG-H1-x samples were 5.9, 7.4, 6.5, 6.3, and 7.1 $\times$ 10^5, corresponding to x = 1, 5, 10, 20, and 30, respectively. The molecular weight of the pure PS sample was measured as 5.5 $\times$ 10^5. These data indicate that the molecular weights of PS in the PS/LDH nanocomposites were comparable to that of the pure PS sample, which indicates that the PS molecular weights in the nanocomposite samples had no considerable effect on the thermal properties of pure PS and the PS/LDH nanocomposites. The enhancement of the thermal properties of the PS/LDH nanocomposites were ascribed to the introduction of the LDH layers into the PS matrix.

CONCLUSIONS

PS/LDH nanocomposites were synthesized successfully via *in situ* emulsion and suspension polymerization with different surfactants and spacers. Completely exfoliated nanocomposites were obtained for the samples with contents of ZnAl LDH no more than 20 wt % with emulsion polymerization and 10 wt % with suspension polymerization when LG surfactant and the long-chain spacer *n*-hexadecane were used. TEM images showed that the exfoliated ZnAl–LDH layers were well dispersed at the molecular level in the PS matrix. However, when SDS surfactant or the short-chain spacer *n*-octane was used, only intercalated or intercalated–exfoliated structures of PS/LDH nanocomposites were obtained, wherein several LDH layers were stacked on each other. The TGA data show that the samples with only a suitable amount of modified LDH had enhanced thermal stability compared with the pure PS. When the 50% weight loss was selected as a comparison point, the thermal decomposition temperature of the exfoliated PS/LDH sample E-LG-H1-5 with 5 wt % LDH was about 28°C higher than that of pure PS. We believe that the *in situ* technique used in this study could be applied to prepare other exfoliated polymer/LDH nanocomposites, such as poly(L-lactide)/LDH, polyacrylate/LDH, and PMMA/LDH nanocomposites.

References

1. Alexandre, M.; Dubois, P. Mater Sci Eng 2000, 28, 1.
2. Kim, Y. K.; Choi, Y. S.; Wang, M. H.; Chung, I. J. Chem Mater 2002, 14, 4990.
3. Vyazovkin, S.; Dranca, I.; Fan, X. W.; Advincula, R. Macromol Rapid Commun 2004, 25, 498.
4. Lu, J.; Zhao, X. P. J. Colloid Interface Sci 2004, 273, 651.
5. Chen, G. X.; Choi, J. B.; Yoon, J. S. Macromol Rapid Commun 2005, 26, 183.
6. Chen, W.; Feng, L.; Qu, B. J. Solid State Commun 2004, 130, 259.
7. Choi, Y. S.; Wang, K. H.; Xu, M. Z.; Chung, I. J. Chem Mater 2002, 14, 2936.
8. Choi, Y. S.; Choi, M. H.; Wang, K. H.; Kim, S. O.; Kim, Y. K.; Chung, I. J. Macromolecules 2001, 34, 8978.
9. Wang, D. Y.; Zhu, J.; Yao, Q.; Wilkie, C. A. Chem Mater 2002, 14, 3837.
10. Xu, M. Z.; Choi, Y. S.; Kim, Y. K.; Wang, K. H.; Chung, I. J. Polymer 2003, 44, 6387.
11. Ding, R. F.; Hu, Y.; Gui, Z.; Zong, R. W.; Chen, Z. Y.; Fan, W. C. Polym Degrad Stab 2003, 81, 473.
12. Essawy, H.; Badran, A.; Youssef, A.; El-Hakim, A. E. Polym Bull 2004, 53, 9.
13. Yeh, J. M.; Liou, S. J.; Lai, M. C.; Chang, Y. W.; Huang, C. Y.; Chen, C. P.; Jaw, J. H.; Tsai, T. Y.; Yu, Y. H. J Appl Polym Sci 2004, 94, 1936.
14. Leroux, F.; Besse, J. P. Chem Mater 2001, 13, 3507.
15. Chen, W.; Qu, B. J. Chem Mater 2003, 15, 3208.
16. Moujahid, E. M.; Besse, J. P.; Leroux, F. J Mater Chem 2002, 12, 3324.
17. Adachi-Pagano, M.; Forano, C.; Besse, J. P. Chem Commun 2000, 1, 91.
18. Kurata, M.; Tsunashima, Y. Polymer Handbook, 4th ed.; Wiley: New York, 1999.
19. Qiu, L. Z.; Chen, W.; Qu, B. J. Polym Degrad Stab 2005, 87, 433.
20. Triantafillidis, C. S.; LeBaron, P. C.; Pinnavaia, T. J. Chem Mater 2002, 14, 4088.
21. Vaia, R. A.; Jandt, K. D.; Kramer, E. J.; Giannelis, E. P. Macromolecules 1995, 28, 8080.
22. Meneghetti, P.; Qutubuddin, S. Langmuir 2004, 20, 3424.
23. Chen, W.; Feng, L.; Qu, B. J. Chem Mater 2004, 16, 368.
24. Chen, W.; Qu, B. J. J Mater Chem 2004, 14, 1705.
25. Paul, M.-A.; Alexandre, M.; Degee, P.; Henrist, C.; Rulmont, A.; Dubois, P. Polymer 2003, 44, 443.